International Journal of Pharmaceutics 636 (2023) 122844

Contents lists available at ScienceDirect

International Journal of Pharmaceutics

journal homepage: www.elsevier.com/locate/ijpharm

Co-delivery of gemcitabine and Triapine by calcium carbonate nanoparticles against chemoresistant pancreatic cancer

Yongmei Zhao [a,1], Yuanlin Zheng [a,1], Yan Zhu [a], Kai Ding [a], Mengjiao Zhou [a,*], Tianqing Liu [b,*]

[a] School of Pharmacy, Nantong University, Nantong, China
[b] NICM Health Research Institute, Western Sydney University, Westmead, Australia

ARTICLE INFO

Keywords:
Calcium carbonate nanoparticles
Gemcitabine
Drug resistance
Triapine
Pancreatic cancer

ABSTRACT

Pancreatic cancer is a malignant disease with high mortality, and its systemic treatment strategy mainly focuses on chemotherapy. Yet, the overall prognosis of pancreatic cancer patients is still extremely poor with a low survival rate. Gemcitabine (GEM) is a widely used chemotherapeutic agent for the treatment of pancreatic cancer. However, GEM chemoresistance remains the major challenge. In this study, we prepared calcium carbonate nanoparticles ($CaCO_3$ NPs) loaded with a nucleotide reductase inhibitor (Triapine) and GEM to suppress the GEM resistance of pancreatic cancer cells (PANC-1/GEM) and solve the problem of poor solubility of Triapine. $CaCO_3$-GEM-Triapine NPs nano-formulations enhanced the therapeutic effect of GEM-based chemotherapy by inhibiting cancer cell proliferation, migration, and resistance to GEM using both 2D PANC-1/GEM cells and 3D tumor spheroids. The study indicated that $CaCO_3$ NPs loaded with GEM and Triapine could provide an effective treatment option to overcome drug resistance in pancreatic cancer.

1. Introduction

Pancreatic cancer is the leading cause of cancer-related deaths worldwide because of its poor prognosis after diagnosis, and the five-year survival rate is about 5% (Rahib et al., 2014; Lambert et al., 2019). Chemotherapy is the commonly used approach for pancreatic cancer treatment. Gemcitabine (GEM), in particular, is a standard-of-care first-line systemic therapy widely used for patients with advanced or metastatic pancreatic cancer (Chin et al., 2018). However, GEM chemoresistance remains the major challenge after initial drug treatment, resulting in reduced survival (Amrutkar and Gladhaug, 2017). Many studies have been conducted to investigate combination therapies with GEM, but no significant therapeutic outcomes have been achieved in clinics so far (Khan et al., 2019). Therefore, finding new approaches or efficient delivery systems that can overcome GEM resistance and improve survival rates is highly needed.

Many factors contribute to GEM resistance via regulation of drug transport, DNA damage and repair, and renewability of cancer stem cells (Chen et al., 2012; Zinzi et al., 2014; Quint et al., 2012; Jia and Xie, 2015; Zeng et al., 2019; Dauer et al., 2017). Among them, ribonucleotide reductase (RR), which functions as a catalyzer to convert ribonucleotides to deoxyribonucleotides during the DNA replication and repair processes, has been shown to play an important role in the development of GEM chemoresistance (Fisher et al., 2013). RR contains two subunits, M1 (RRM1) and M2 (RRM2), which have been proven to affect the adjuvant therapy of pancreatic cancer. (Fisher et al., 2013) Specifically, RRM2 expression level has a positive relationship with DNA damage repair and replication (Itoi et al., 2007; Fujita et al., 2010). High level of RRM2 expression is associated with a poor response to GEM-based chemotherapy, leading to a poor prognosis (Zhan et al., 2021). Our previous study has demonstrated that deferasirox-induced inhibition of RRM2 expression significantly enhanced the GEM chemosensitivity (Zhao et al., 2021). Therefore, inhibition of RRM2 may be one effective method to improve the anticancer activity of chemotherapy. Triapine, as an iron-binding compound and anticancer thiosemicarbazone, acts as a human ribonucleotide reductase (RNR) inhibitor by consuming large amounts of deoxy-ribonucleoside triphosphate (dNTP) and selectively blocking the synthesis of nucleotides needed for DNA synthesis and replication in cancer cells (Aye et al., 2012; Plamthottam et al., 2019). Moreover, Triapine can directly quench the tyrosine diiron group on the M2 subunit by reducing the iron complex and giving an electron, thus inhibiting the expression of RRM2 (Enyedy

* Corresponding authors.
E-mail addresses: mjzhou0207@ntu.edu.cn (M. Zhou), michelle.tianqing.liu@gmail.com (T. Liu).
[1] Equally contributed.

https://doi.org/10.1016/j.ijpharm.2023.122844
Received 8 October 2022; Received in revised form 14 February 2023; Accepted 11 March 2023
Available online 14 March 2023

et al., 2011; Mortazavi et al., 2013). A phase 1 trial study found that combining Triapine with GEM improved anticancer efficacy in patients who had previously failed gemcitabine treatment. (Fischer et al., 2016) However, the poor solubility and short plasma half-life of Triapine limit its application against GEM-resistant cancer. (Zhao et al., 2022) Thus, it is urgent to develop an ideal platform for effectively delivering it to tumor sites.

Calcium carbonate nanoparticles ($CaCO_3$ NPs) have been widely used in in many biomedical applications including drug delivery and diagnosis due to their advantages including biocompatibility, low toxicity, low immune response, pH sensitivity, and environment friendly. (Wei et al., 2008) $CaCO_3$ NPs can increase the solubility, stability, and circulation half-life of the drug cargos, particularly for water-insoluble drugs. (Zhou et al., 2019) $CaCO_3$ NPs are stable at neutral pH and decompose into Ca^{2+} and CO_2 at acidic pH. Thus, this pH-responsive drug delivery is suitable for the delivery of chemotherapeutic drugs to the tumor regions because of the acidic tumor microenvironment.

In this study, $CaCO_3$ NPs were used as a drug nanocarrier to load Triapine and GEM. The drug-encapsulated $CaCO_3$ NPs ($CaCO_3$-GEM-Triapine NPs) improved the chemosensitivity of GEM in GEM-resistant pancreatic cancer cells, while increasing drug accumulation in the acidic tumor microenvironment. Our results showed that the $CaCO_3$-GEM-Triapine NPs synergistically improved the therapeutic efficiency against GEM-resistant pancreatic cancer cells by inhibiting pancreatic cancer cell proliferation, limiting cancer cell migration, and reducing 3D tumor spheroid growth.

2. Materials and methods

2.1. Cell culture

Human pancreatic cancer cells (PANC-1) were purchased from the National Collection of Authenticated Cell Cultures, China. Cells were cultured in Dulbecco's Modified Eagle Medium (DMEM, Thermo Fisher Scientific), supplemented with 10% fetal bovine serum (FBS, Thermo Fisher Scientific) and 1% penicillin–streptomycin (Sigma-Aldrich). Drug resistance of pancreatic cancer cells (PANC-1/GEM) were cultured in low calcium carbonate DMEM supplemented with10% FBS and 1% penicillin–streptomycin and induced by 18 μg / mL GEM (Sigma-Aldrich) for ten months. Both PANC-1 and PANC-1/GEM were cultured in a 37 ℃ humidified incubator containing 5% CO_2.

2.2. Drug loading and quantification

A certain amount of GEM (15 mg), Tripaine (60 ug), and $CaCl_2$ (25 mg) were dissolved in methanol. The mixed solution and NH_3HCO_3 were put into a vacuum drying box for 24 h and then centrifuged for 7000 g/min for 10 min to precipitate, wash with methanol, and repeat the above steps three times (Liu et al., 2014). The drug entrapment efficiency was calculated by the standard curve. The UV absorption peaks of GEM and Triapine are at 275 nm and 360 nm, respectively.

$$\textit{Drug entrapment}: \frac{\text{Total amount of drugs - Amount of drugs in the supernatant}}{\text{Total amount of drugs}} \times 100\%$$

The morphology of $CaCO_3$-GEM-Triapine NPs was characterized by a transmission electron microscope (TEM, Talos F200X, Thermo Fisher Scientific). The particle size and zeta potential of $CaCO_3$-GEM-Triapine NPs were measured by dynamic light scattering (DLS, Nano-zs30, Malvern Panalytical).

2.3. Release profile of GEM or Tripaine from $CaCO_3$-GEM-Triapine NPs

To measure the drug release profiles, the dialysis bag (MWCO 3000 Da) containing $CaCO_3$-GEM-Triapine NPs was placed in a 500 mL beaker containing pH 5.7 and pH 7.4 buffers respectively, and the dialysis device was placed at 37 ℃ at 100 rpm. Samples were collected at different time points (0.5, 2, 4, 6, 8, 10, 12, and 24 h), and the release amount was calculated according to the standard curve. Due to the poor water solubility of Triapine, the drug release measurement was carried out using a Xilin bottle on a constant temperature shaker at 37 ℃ for 24 h. The percent drug release was calculated and presented as a Triapine drug release profile. All release experiments are in triplicate.

2.4. Cell viability and drug combination studies

The cytotoxicity of $CaCO_3$-GEM-Triapine NPs was determined by MTT assay. PANC-1 cells and PANC-1/GEM cells were seeded into a 96-well plate at a concentration of 1×10^4 cells/well and incubated at 37 °C with 5% CO_2 for 24 h. The cells were treated with $CaCO_3$ NPs, GEM, Triapine, GEM&Triapine, and $CaCO_3$-GEM-Triapine NPs at corresponding concentrations of GEM (18 μg/mL) and Triapine (0.21 μg/mL) for 48 h, followed by 20 uL of MTT in each well and incubated at 37 °C for another 4 h. They were washed with PBS and dissolved in 100 μL dimethyl sulfoxide per well. The absorbance was then measured at 490 nm using a microplate reader (Thermo Fisher Scientific).

PANC-1 cells were seeded into 96-well culture plates with a density of 1×10^4 cells per well. After 24 h incubation, GEM and Triapine with different molar ratios (R) were added to the cells, and the synergistic effect was evaluated using Chou and Talalay's combination Index (CI). The CI values for synergism, synergism, and antagonism were$<$1, equal to 1, and greater than 1, respectively.

2.5. Multidrug resistance (MDR) study

MDR was studied by measuring drug efflux activity using the Vybrant Multidrug Resistance Assay (Thermo Fisher Scientific). The fluorescent dye Calcein acetoxymethyl ester (Calcein AM) was used as the substrate of p-glycoprotein efflux activity. MDR cells expressing high levels of p-glycoprotein can rapidly secrete non-fluorescent Calcein AM from the plasma membrane, thereby reducing the accumulation of fluorescent Calcein in the cytoplasm. The cells were added to the 96-well plate at a density of 5×10^5 cells per well and treated with verapamil (Thermo Fisher Science), Calcein (Thermo Fisher Science), and $CaCO_3$ NPs, GEM, Triapine, GEM&Triapine, and $CaCO_3$-GEM-Triapine NPs. The retention rate of Calcein was measured by a microplate reader. The specific fluorescence absorption peak of Calcein was 494 nm and the emission peak was 517 nm.

2.6. Cell migration assay

PANC-1 and PANC-1/GEM cells were seeded in a 6-well plate, respectively. After cell density reached 80%, the wounds on the cell monolayers were made using sterile pipette tips. The cells were treated with $CaCO_3$ NPs, GEM, Triapine, GEM&Triapine, and $CaCO_3$-GEM-Triapine NPs, and cell migration and wound closure was recorded at 0 h and 24 h. The results were analyzed with the Image J software.

2.7. Western blotting

The expression of the target protein RRM2 was assessed by western blotting. The treated PANC-1 cells were harvested, and the total proteins were extracted and quantitatively detected by the bicinchoninic acid protein assay (BCA) kit (Beyotime). Protein samples were prepared at a concentration of 50 μg protein/20 μL. After electrophoresis of the prepared samples in loading buffer on SDS-PAGE gels, the samples were transferred to a PVDF membrane and incubated with a blocking solution at room temperature. The membrane was first treated with an anti-RRM2 antibody (1:1000, Abcam) or an anti-β-actin monoclonal antibody (1:1000, Abcam) overnight at 4 ℃. After proper washing, the membrane was incubated with the secondary antibodies at room

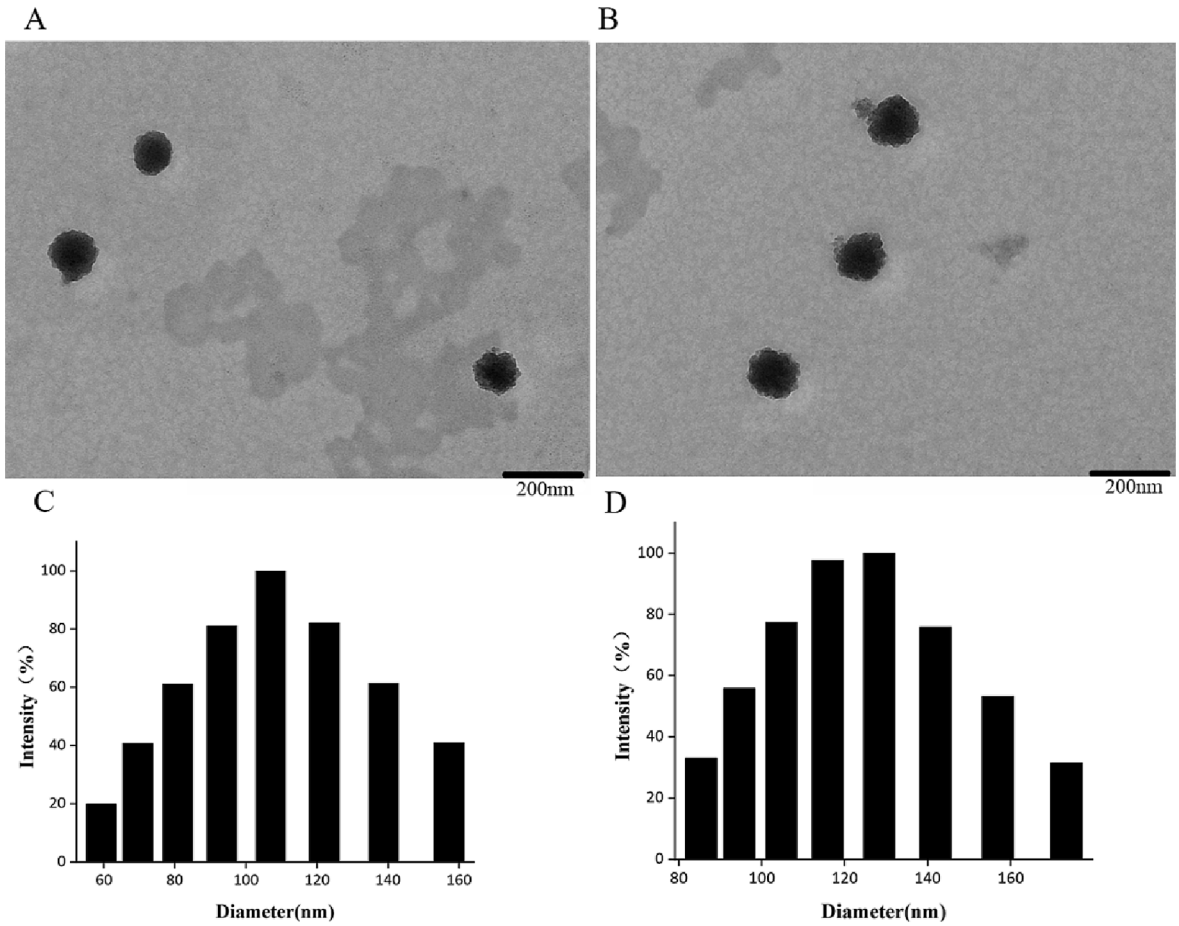

Fig. 1. Characterization of $CaCO_3$ NPs with or without drug loading: TEM images of (A) $CaCO_3$ NPs and (B) $CaCO_3$-GEM-Triapine NPs and the TEM particle size data of (C) $CaCO_3$ NPs, and (D) $CaCO_3$-GEM-Triapine NPs, which were converted directly to cumulative number-based distributions.

temperature in the dark for 1 h. The protein bands were scanned with the Odyssey imaging system (LI-COR, LI-COR Biosciences) after washing and drying. The intensity was quantified and analyzed via image J.

2.8. Inhibition of 3D PANC-1/GEM tumor spheroids

PANC-1/GEM tumor spheroids were cultured in a microwell device using our established method. (Liu et al., 2014; Yao et al., 2014) The formation of the tumor spheroids was monitored by an optical microscope (CKX53, OLYMPUS). When the diameter of the tumor spheroids reached 200 μm, they were treated with $CaCO_3$ NPs, GEM, Triapine, GEM&Triapine, and $CaCO_3$-GEM-Triapine NPs for 7 days (Zhao et al., 2021). The size of the spheroids was recorded, and the roundness was calculated using the following formula: roundness (%) = 100 − (R − r)/R × 100 (R: represents the radius of the minimum circumscribed circle; r: represents the maximum inscribed concentric circle) and analyzed by Image J (Seo et al., 2021). In addition, the tumor spheroid volume was calculated with the following formula: $V = (\pi \times d_{max} \times d_{min})/6$, and the change ratio of the tumor spheroid volume was compared with the initial volume of each group [29].

2.9. Statistical analysis

All experiments are performed three times and carried out using t-tests via GraphPad Prism version 9. All data are shown as mean ± standard deviations. *$p < 0.05$, ** $p < 0.01$, and *** $p < 0.001$ were considered statistically significant.

Table 1
Physical properties and drug loading efficiency of $CaCO_3$ NPs and $CaCO_3$-GEM-Triapine NPs.

Sample	Hydrodynamic Size (nm)	Zeta-Potential (mV)	Polydispersity Index	Entrapment efficiency (%)
$CaCO_3$ NPs	106.4 ± 5.5 nm	−8.23 ± 1.03	0.203	–
$CaCO_3$-GEM-Triapine NPs	128.8 ± 7.1 nm	−5.46 ± 1.98	0.216	82 ± 3.5 (GEM) 76 ± 2.4 (Triapine)

3. Results and discussion

3.1. Preparation and characterization of $CaCO_3$-GEM-Triapine NPs

$CaCO_3$ NPs loaded with GEM and Triapine was prepared by a simple coprecipitation method. $CaCO_3$ NPs and $CaCO_3$-GEM-Triapine NPs were characterized by evaluating its morphology, hydrodynamic size, surface charge, and loading efficiency. The morphologies of $CaCO_3$ NPs and $CaCO_3$-GEM-Triapine NPs were measured by TEM, and the results revealed that they were both uniform spheres (Fig. 1). The hydrodynamic dimensions of $CaCO_3$ NPs and $CaCO_3$-GEM-Triapine NPs were studied by DLS analysis. The results showed that the size of $CaCO_3$ NPs was 106.4 ± 5.5 nm, while the size of $CaCO_3$-GEM-Triapine NPs was increased to 128.8 ± 7.1 nm (Table1). The loading efficiency was determined using a UV spectrophotometer, and the standard curve was

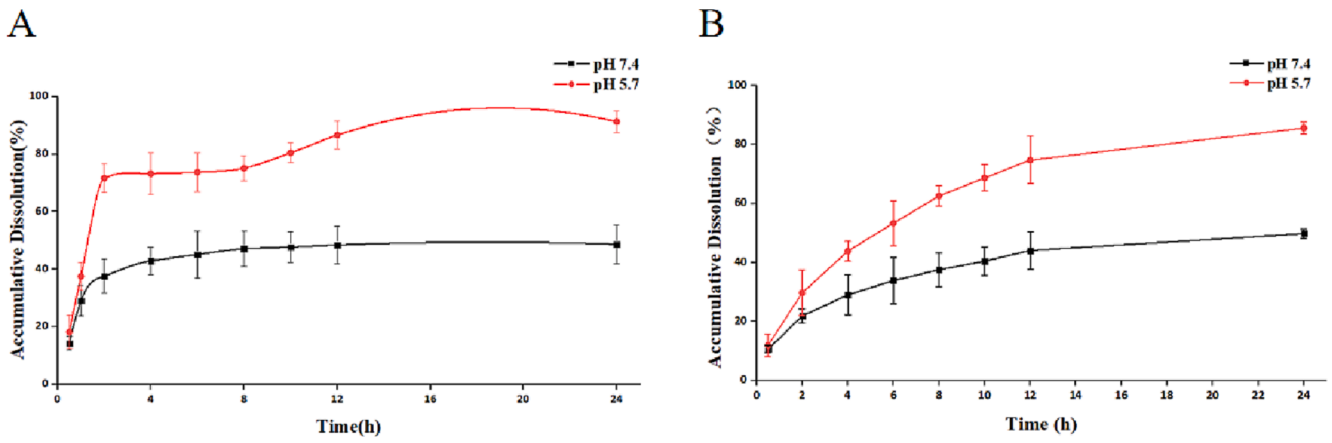

Fig. 2. (A)The dissolution curve of GEM in $CaCO_3$-GEM-Triapine NPs in the buffer of pH 5.7 and pH 7.4, and (B) the dissolution curve of Triapine in the buffer of pH 5.7 and pH 7.4, each point represents the mean value ± SD (n = 3).

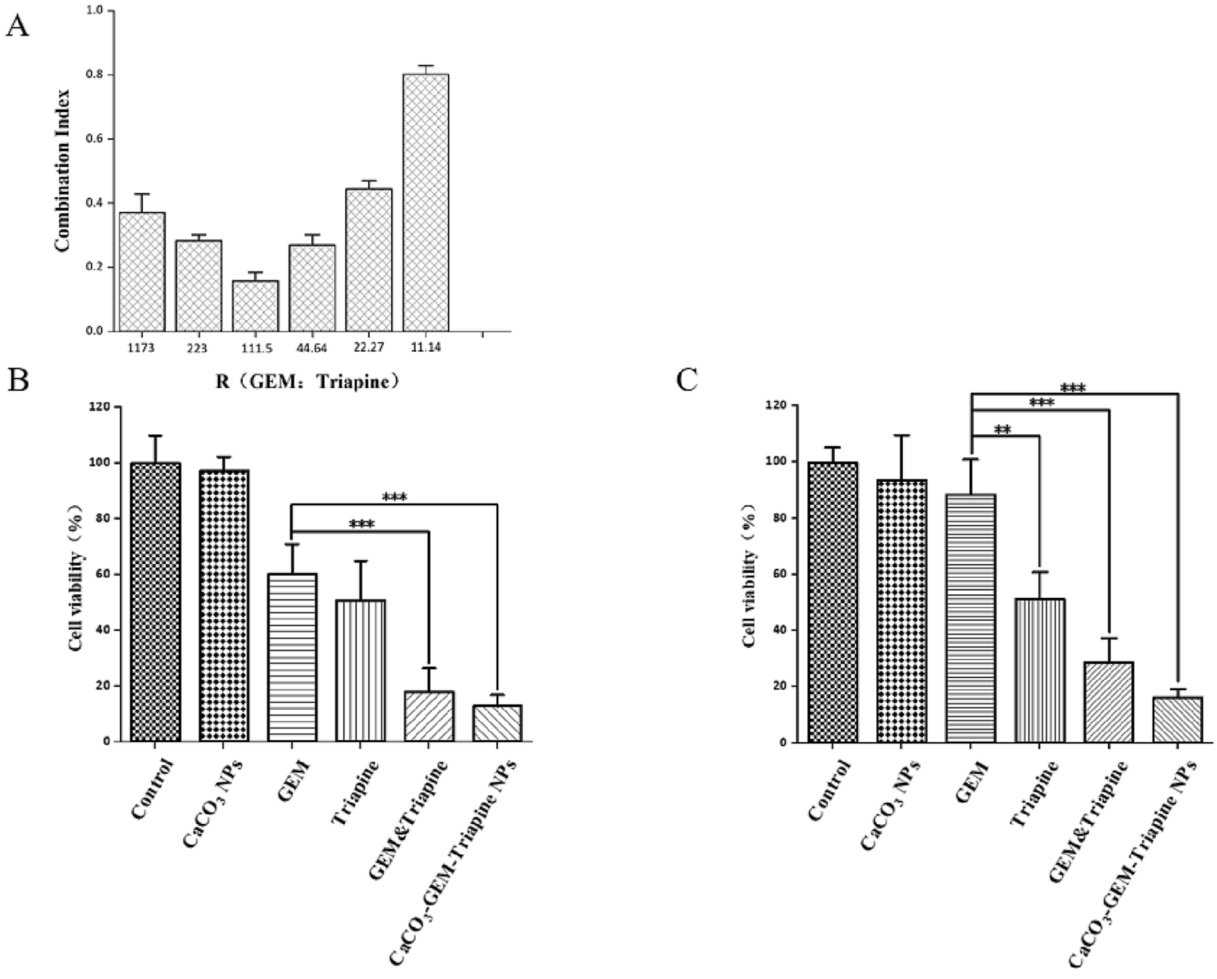

Fig. 3. (A) PANC-1 cells were treated with different molar ratios of GEM and Triapine. Drug concentrations are selected such that at least one individual drug dose inhibits cell growth by 40% to 60%. Combination index (CI) values were calculated for GEM and Triapine treatments. (B) PANC-1 cells and (C) PANC-1/GEM cells were treated with $CaCO_3$ NPs, GEM, Triapine, GEM&Triapine, and $CaCO_3$-GEM-Triapine NPs respectively for the MTT study. (** $p < 0.01$, *** $p < 0.001$).

obtained by measuring the absorbance values of GEM and Triapine at the peak at 275 nm and 360 nm, respectively. According to the calculation, the encapsulation efficiency of GEM and Triapine was about 82% and 76% respectively, which was shown in Table 1.

The release kinetics of the GEM and Triapine from $CaCO_3$-GEM-Triapine NPs was investigated over time in PBS buffer at 37 °C, and the results are summarized in Fig. 2. $CaCO_3$-GEM-Triapine NPs had a pH-dependent release pattern, according to the release study. As shown in Fig. 2A, when tested at pH 5.7, GEM was rapidly released within 2 h. However, <50% of GEM was release after 24 h at pH 7.4. Due to the poor water solubility of Triapine, the superposition method was adopted to calculate the release amount in order to accurately calculate the amount

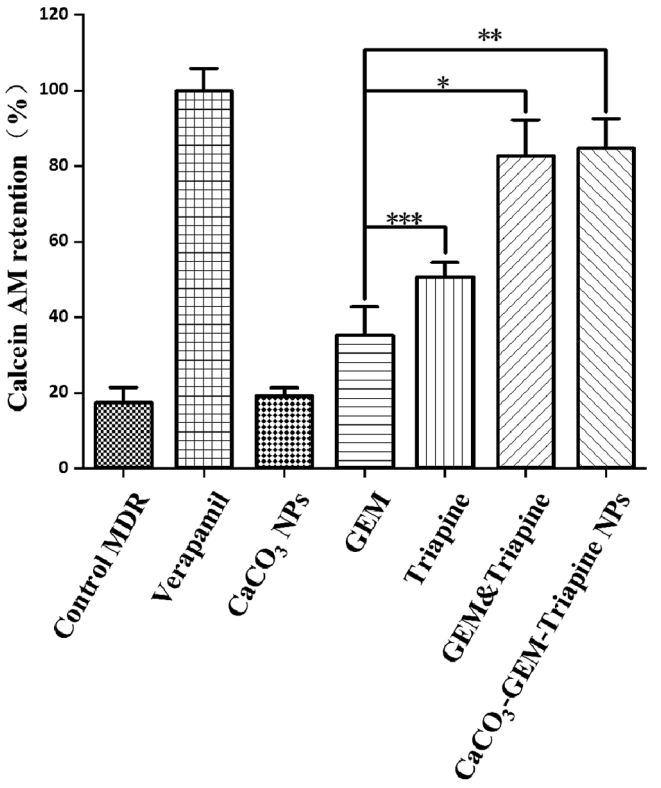

Fig. 4. The multidrug resistance of PANC-1/GEM cells to GEM was studied in the treatment groups of $CaCO_3$ NPs, GEM, Triapine, GEM&Triapine, and $CaCO_3$-GEM-Triapine NPs and compared with blank control and positive control. (* $p < 0.05$, ** $p < 0.01$, *** $p < 0.001$).

of Triapine in the buffer. As shown in Fig. 2B, Triapine was released uniformly over time. According to the general trend of Triapine release, its release amount at pH 5.7 was significantly greater than that at pH 7.4. This phenomenon is similar to the GEM release pattern, demonstrating that the $CaCO_3$ NPs nanocarrier has a certain pH responsiveness.

3.2. Drug combination study and in vitro cell viability study

The synergistic cytostatic effect of GEM and Triapine on PANC-1/GEM cells was tested after 72 h of co-incubation (Fig. 3A). Synergistic effect was quantified by calculated the combination index (CI). CI values<1 indicated synergy, while values greater than 1 indicated antagonism. The synergistic effect was greatest when the drug molar ratio (R) (GEM:Triapine) was 111.5. The reason for the drug interaction may be that Triapine directly quenches the tyrosine diiron group on the M2 subunit by reducing iron complex and directly quenches the diiron group of tyrosine, inhibiting the expression of RRM2, thus blocking the repair and replication of DNA damage, and enhancing the therapeutic effect of GEM.

The cytotoxicity of $CaCO_3$-GEM-Triapine NPs was tested in both PANC-1 and drug-resistant PANC-1/GEM cells. According to the results of MTT assay, $CaCO_3$ NPs had no significant cytotoxic effect on PANC-1 and PANC-1/GEM cells (Fig. 3). Free GEM had more cytotoxicity to PANC-1 cells than the control group, while it was not significantly toxic to PANC-1/GEM cells. Both cells were affected by free Triapine and reduced their survival rates to about 50%. The cell viability of the GEM&Triapine group to PANC-1 and PANC-1/GEM cells was around 20–30%, indicating that combination of Triapine and GEM inhibited resistance of PANC cells to GEM to some extent. In addition, compared with the free GEM&Triapine group, the $CaCO_3$-GEM-Triapine NPs group had a better curative effect, which could be attributed to the improved solubility of Triapine by the formulation.

3.3. Anti-MDR effects

MDR is commonly associated with the overexpression of transmembrane transporter P-glycoprotein (P-gp). P-gp can overcome the influx driven by passive diffusion of cytotoxic drugs by pumping these drugs out of the cell. Therefore, inhibiting the expression of P-gp is an effective way to enhance the sensitivity of PANC-1/GEM to GEM. As shown in Fig. 4, the AM retention rate of Calcein in $CaCO_3$ NPs and blank control was relatively low, whereas it was slightly increased in the GEM treatment group. The Calcein AM retention rate in the Triapine group reached 50.7%. Compared with verapamil, positive control of P-gp inhibitors, the retention rate of Calcein AM was significantly increased to 84.8% when treated with $CaCO_3$-GEM-Triapine NPs. These findings suggest that the treatment of $CaCO_3$-GEM-Triapine NPs can inhibit the P-gp expression in PANC-1/GEM cells and increase the accumulation of drugs in the cells.

3.4. Cell migration

We used the cell scratch test to study the ability of cell migration *in vitro*. As shown in Fig. 5, $CaCO_3$ NPs have no significant effect on cell migration. When treated with free GEM, Triapine, GEM&Triapine, the migration rate of PANC/GEM cells showed slightly reduced compared to control group. In contrast, PANC/GEM cells which received $CaCO_3$-GEM-Triapine NPs treatment had the best inhibitory effect on cell migration compared to other treated groups. These results suggest that $CaCO_3$-GEM-Triapine NPs dramatically inhibited the invasiveness of GEM-resistant pancreatic cancer cells.

3.5. Expression of drug resistance-related proteins

To study the mechanism and effect in suppressing GEM resistance after $CaCO_3$-GEM-Triapine NPs treatment, the protein expression of RRM2 and actin was detected by western blotting. In Fig. 6A and B, the $CaCO_3$-GEM-Triapine NPs group had the lowest RRM2 band intensity of any treatment groups, indicating that the expression of RRM2 protein was significantly down-regulated in $CaCO_3$-GEM-Triapine NPs treated cells. It is expected that Triapine directly quenched the tyrosine diiron group on the M2 subunit and inhibited RRM2 expression. In summary, these data showed that $CaCO_3$-GEM-Triapine NPs significantly reduced RRM2 expression, which could overcome GEM resistance of cancer cells and improve the treatment outcomes of GEM-resistant pancreatic cancer.

3.6. Tumor spheroid assay

The anticancer effect was further evaluated using the 3D tumor spheroid model, which has been widely used for anticancer drug screening due to its better simulation of the physiological properties of tumor tissues. After the establishment of the PANC-1/GEM tumor spheroid model, different treatments were administered, and changes of spheroid morphologies were monitored (Fig. 7A). As shown in Fig. 7B, $CaCO_3$ NPs had no obvious effect on the volume of PANC-1/GEM tumor spheroids. Meanwhile, the of GEM&Triapine and $CaCO_3$-GEM-Triapine NPs had higher therapeutic effects on tumor spheroids than those of the other groups.

On the 7th day, the change rates of tumor spheroid volume in control, $CaCO_3$ NPs, GEM, Triapine, GEM&Triapine and $CaCO_3$-GEM-Triapine NPs groups were 466.4 ± 57.4%, 475.7 ± 17.8%, 407.8 ± 29.5%, 301.8 ± 30.4%, 102.7 ± 18.0%, 16.9 ± 5.0%, respectively. $CaCO_3$-GEM-Triapine NPs showed the most potent inhibitory effect on the growth of PANC-1/GEM tumor spheroids. In the roundness analysis, we found that when $CaCO_3$-GEM-Triapine NPs were used, the periphery of the tumor spheroids was more likely to be broken into irregular shapes (Fig. 6C). These discoveries are consistent with the data based on 2D cells. Our results demonstrated that $CaCO_3$-GEM-Triapine NPs were

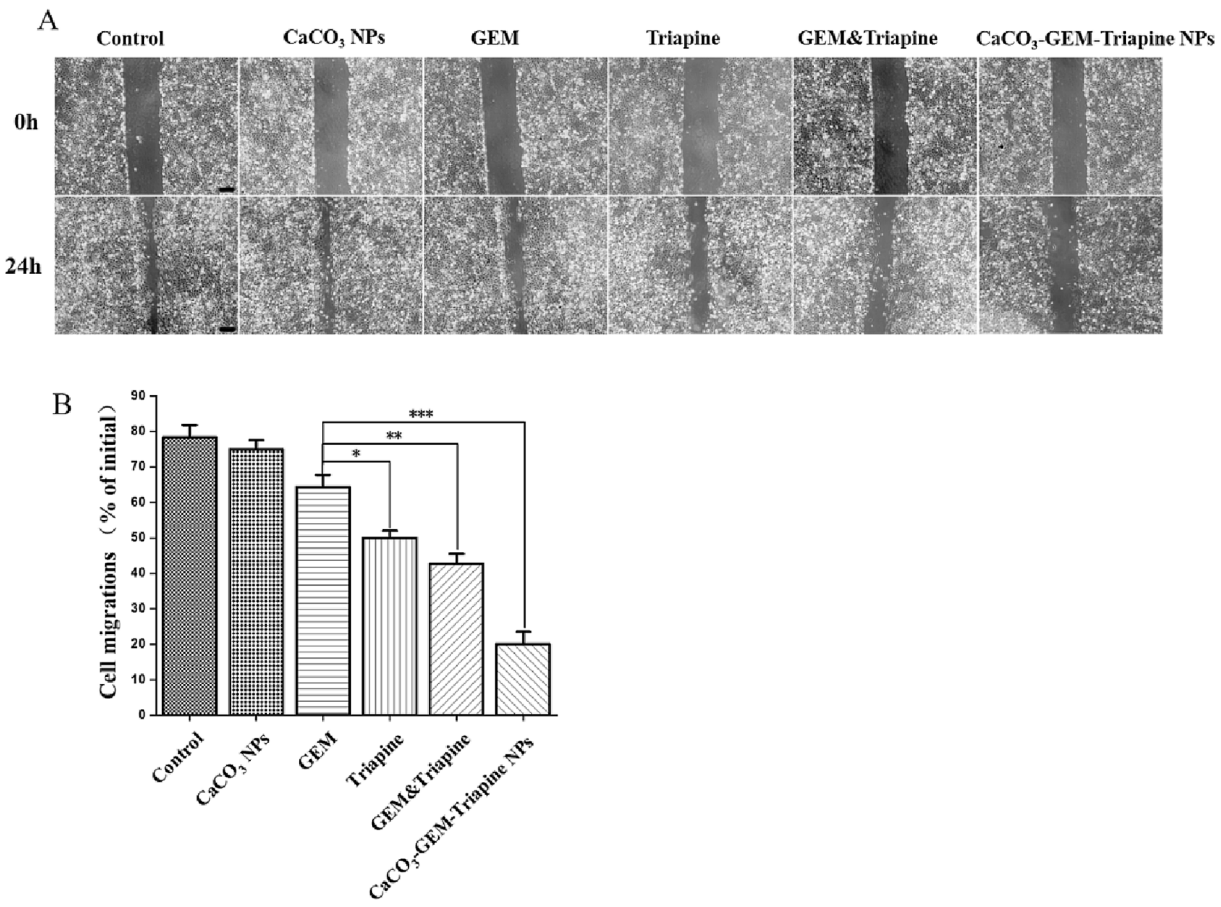

Fig. 5. (A) The images of PANC-1/GEM cells under the treatments of $CaCO_3$ NPs, GEM, Triapine, GEM&Triapine, and $CaCO_3$-GEM-Triapine NPs. Scale bar 100 um (B) The migration rates of PANC-1/GEM cells treated with different samples. (* $p < 0.05$, ** $p < 0.01$, *** $p < 0.001$).

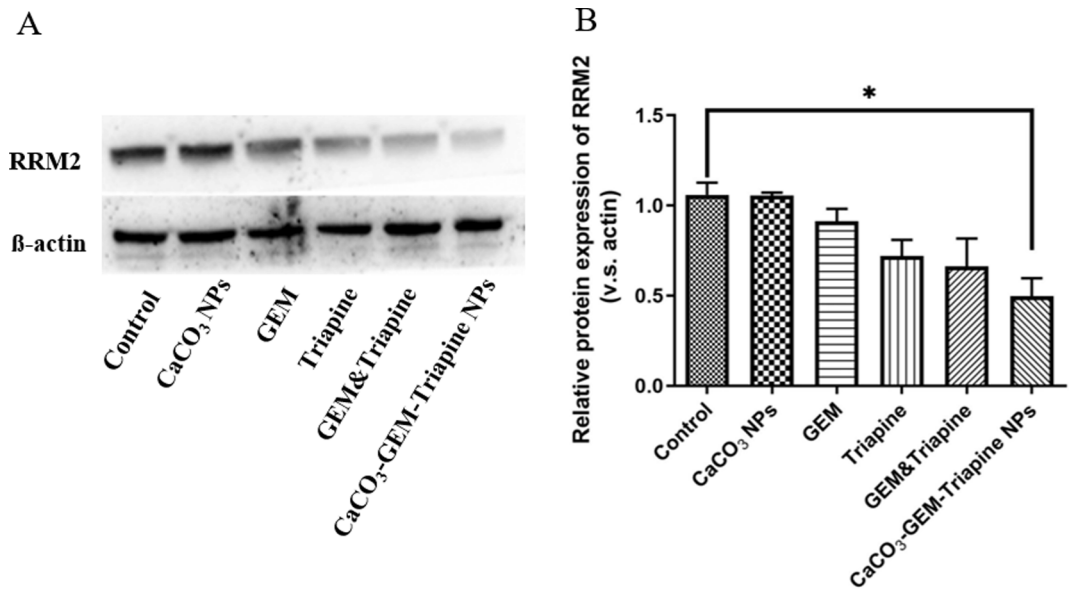

Fig. 6. (A) Western blot of RRM2 and actin expression in PANC-1/GEM cells at 24 h post-treatment. (B) Relative expression level of RRM2 in PANC-1/GEM cells after different treatments. (* $p < 0.05$).

more effective in inhibiting the formation and growth of PANC-1/GEM tumor spheroids than free drugs, suggesting that $CaCO_3$-GEM-Triapine NPs significantly improved the therapeutic efficacy of GEM chemotherapy against PANC-1/GEM cells *in vitro* by inducing the death of PANC-1/GEM cells and reducing the drug tolerance of PANC-1/GEM cells.

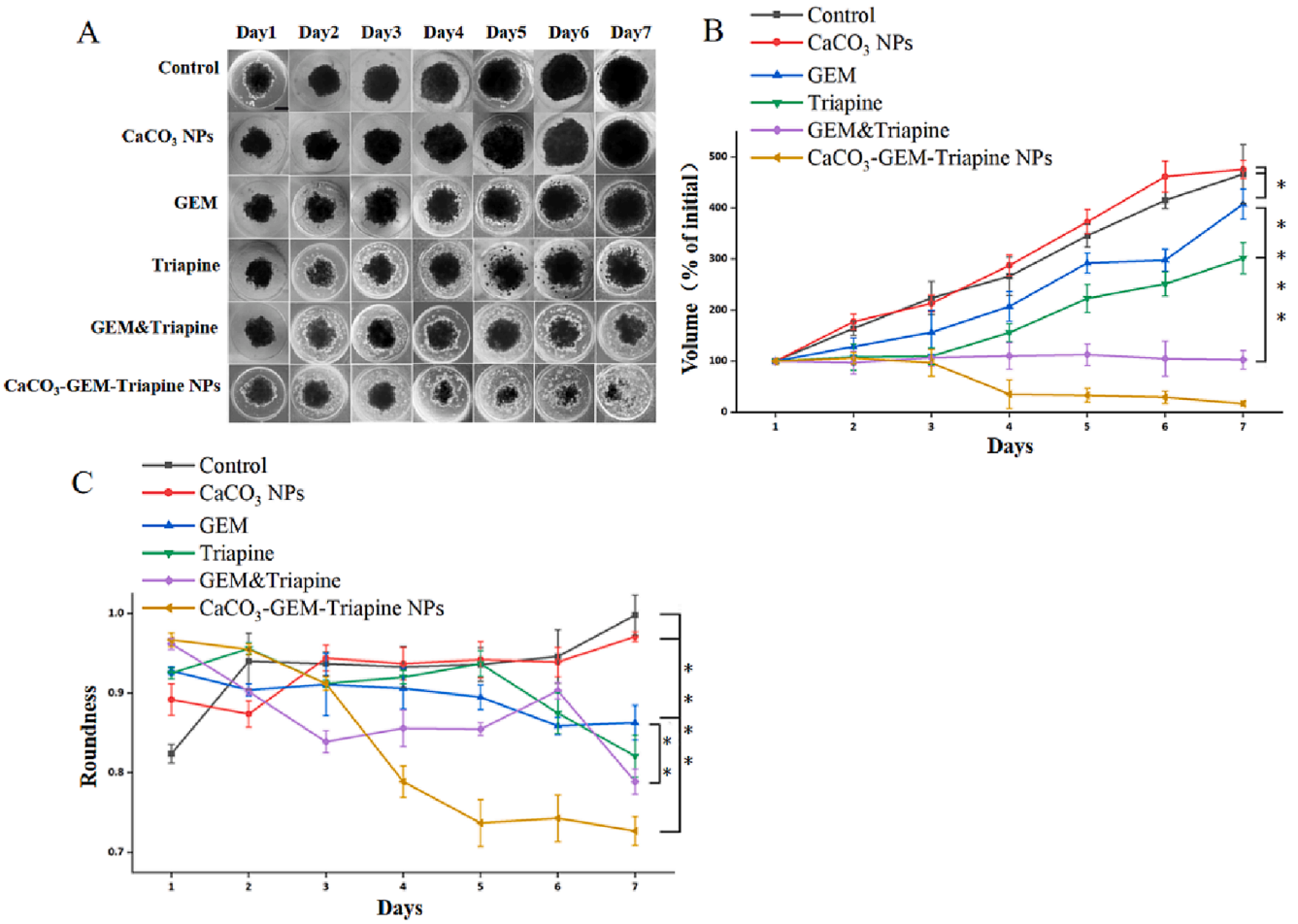

Fig. 7. (A) Morphology of 3D PANC-1/GEM tumor spheroids treated with blank control, $CaCO_3$ NPs, GEM, Triapine, GEM&Triapine, and $CaCO_3$-GEM-Triapine NPs at the indicated concentration for 7 days. Scale bar: 200 μm. (B) Inhibitory effect on the growth of PANC-1/GEM tumor spheroids. (C) PANC-1/GEM tumor spheroid roundness after treatments, calculated by Image J. (* $p < 0.05$, ** $p < 0.01$).

4. Conclusions

Our study showed that $CaCO_3$-GEM-Triapine NPs enhanced the cytotoxicity of GEM to PANC-1/GEM cells. Its mechanism of action is related to the inhibition of DNA damage repair and replication by Triapine-induced downregulation of RRM2. We also investigated the anticancer effect of $CaCO_3$-GEM-Triapine NPs using a three-dimensional tumor spheroid model. The experiments showed that $CaCO_3$-GEM-Triapine NPs effectively inhibited the formation and growth of PANC-1/GEM tumor spheroids compared with other treatment groups. In conclusion, this study suggests that $CaCO_3$-GEM-Triapineis NPs an effective therapeutic strategy for GEM-resistant pancreatic tumors, offering a novel approach to overcome drug resistance for pancreatic cancer in the clinic.

Declaration of Competing Interest

The authors declare that they have no known competing financial interests or personal relationships that could have appeared to influence the work reported in this paper.

Data availability

Data will be made available on request.

Acknowledgments

Dr. Tianqing Liu is supported by the National Health and Medical Research Council (NHMRC) Early Career Fellowship (Grant No. 1112258) and WSU Vice-Chancellor's Senior Research Fellow. Dr. Yongmei Zhao is supported by the National Science Foundation of the Jiangsu Higher Education Institutions of China (Grant No. 19KJD350002) and Jiangsu's Mass Entrepreneurship and Innovation Program and the Large Instruments Open Foundation of Nantong University (KFJN2063).

References

Amrutkar, M., Gladhaug, I.P., 2017. Pancreatic cancer chemoresistance to gemcitabine. Cancers (Basel) 9, 11.

Aye, Y., Long, M.J.C., Stubbe, J., 2012. Mechanistic studies of semicarbazone triapine targeting human ribonucleotide reductase in vitro and in mammalian cells: tyrosyl radical quenching not involving reactive oxygen species. J. Biol. Chem. 287 (42), 35768–35778.

Chen, M., Xue, X., Wang, F., An, Y., Tang, D., Xu, Y., Wang, H., Yuan, Z., Gao, W., Wei, J., Zhang, J., Miao, Y., 2012. Expression and promoter methylation analysis of ATP-binding cassette genes in pancreatic cancer. Oncol. Rep. 27 (1), 265–269.

Chin, V.; Nagrial, A.; Sjoquist, K.; O'Connor, C. A.; Chantrill, L.; Biankin, A. V.; Scholten, R. J.; Yip, D., Chemotherapy and radiotherapy for advanced pancreatic cancer. *Cochrane Database Syst Rev* **2018,** *3* (3), Cd011044.

Dauer, P., Nomura, A., Saluja, A., Banerjee, S., 2017. Microenvironment in determining chemo-resistance in pancreatic cancer: Neighborhood matters. Pancreatology 17 (1), 7–12.

Enyedy É, A.; Primik, M. F.; Kowol, C. R.; Arion, V. B.; Kiss, T.; Keppler, B. K., Interaction of Triapine and related thiosemicarbazones with iron(III)/(II) and gallium(III): a comparative solution equilibrium study. *Dalton Trans* **2011,** *40* (22), 5895-905.

Fischer, B., Kryeziu, K., Kallus, S., Heffeter, P., Berger, W., Kowol, C.R., Keppler, B.K., 2016. Nanoformulations of anticancer thiosemicarbazones to reduce methemoglobin formation and improve anticancer activity. RSC Adv. 6 (61), 55848–55859.

Fisher, S. B.; Patel, S. H.; Bagci, P.; Kooby, D. A.; El-Rayes, B. F.; Staley, C. A., 3rd; Adsay, N. V.; Maithel, S. K., An analysis of human equilibrative nucleoside transporter-1, ribonucleoside reductase subunit M1, ribonucleoside reductase subunit M2, and excision repair cross-complementing gene-1 expression in patients with resected pancreas adenocarcinoma: implications for adjuvant treatment. *Cancer* **2013,** *119* (2), 445-53.

Fujita, H., Ohuchida, K., Mizumoto, K., Itaba, S., Ito, T., Nakata, K., Yu, J., Kayashima, T., Souzaki, R., Tajiri, T., Manabe, T., Ohtsuka, T., Tanaka, M., 2010. Gene expression levels as predictive markers of outcome in pancreatic cancer after gemcitabine-based adjuvant chemotherapy. Neoplasia 12 (10), 807–817.

Itoi, T., Sofuni, A., Fukushima, N., Itokawa, F., Tsuchiya, T., Kurihara, T., Moriyasu, F., Tsuchida, A., Kasuya, K., 2007. Ribonucleotide reductase subunit M2 mRNA expression in pretreatment biopsies obtained from unresectable pancreatic carcinomas. J Gastroenterol 42 (5), 389–394.

Jia, Y., Xie, J., 2015. Promising molecular mechanisms responsible for gemcitabine resistance in cancer. Genes Dis 2 (4), 299–306.

Khan, S., Setua, S., Kumari, S., Dan, N., Massey, A., Hafeez, B.B., Yallapu, M.M., Stiles, Z. E., Alabkaa, A., Yue, J., Ganju, A., Behrman, S., Jaggi, M., Chauhan, S.C., 2019. Superparamagnetic iron oxide nanoparticles of curcumin enhance gemcitabine therapeutic response in pancreatic cancer. Biomaterials 208, 83–97.

Lambert, A., Schwarz, L., Borbath, I., Henry, A., Van Laethem, J.L., Malka, D., Ducreux, M., Conroy, T., 2019. An update on treatment options for pancreatic adenocarcinoma. Ther. Adv. Med. Oncol. 11.

Liu, T., Winter, M., Thierry, B., 2014. Quasi-spherical microwells on superhydrophobic substrates for long term culture of multicellular spheroids and high throughput assays. Biomaterials 35 (23), 6060–6068.

Liu, T., Kempson, I., de Jonge, M., Howard, D.L., Thierry, B., 2014. Quantitative synchrotron X-ray fluorescence study of the penetration of transferrin-conjugated gold nanoparticles inside model tumour tissues. Nanoscale 6 (16), 9774–9782.

Mortazavi, A., Ling, Y., Martin, L.K., Wei, L., Phelps, M.A., Liu, Z., Harper, E.J., Ivy, S.P., Wu, X., Zhou, B.S., Liu, X., Deam, D., Monk, J.P., Hicks, W.J., Yen, Y., Otterson, G.A., Grever, M.R., Bekaii-Saab, T., 2013. A phase I study of prolonged infusion of triapine in combination with fixed dose rate gemcitabine in patients with advanced solid tumors. Invest New Drugs 31 (3), 685–695.

Plamthottam, S., Sun, D., Van Valkenburgh, J., Valenzuela, J., Ruehle, B., Steele, D., Poddar, S., Marshalik, M., Hernandez, S., Radu, C.G., Zink, J.I., 2019. Activity and electrochemical properties: iron complexes of the anticancer drug triapine and its analogs. J. Biol. Inorg. Chem. 24 (5), 621–632.

Quint, K., Tonigold, M., Di Fazio, P., Montalbano, R., Lingelbach, S., Rückert, F., Alinger, B., Ocker, M., Neureiter, D., 2012. Pancreatic cancer cells surviving gemcitabine treatment express markers of stem cell differentiation and epithelial-mesenchymal transition. Int J Oncol 41 (6), 2093–2102.

Rahib, L., Smith, B.D., Aizenberg, R., Rosenzweig, A.B., Fleshman, J.M., Matrisian, L.M., 2014. Projecting cancer incidence and deaths to 2030: the unexpected burden of thyroid, liver, and pancreas cancers in the United States. Cancer Res 74 (11), 2913–2921.

Seo, J., Kim, K.S., Park, J.W., Cho, J.Y., Chang, H., Fukuda, J., Hong, K.Y., Chun, Y.S., 2021. Metastasis-on-a-chip reveals adipocyte-derived lipids trigger cancer cell migration via HIF-1alpha activation in cancer cells. Biomaterials 269, 120622.

Wei, W., Ma, G.H., Hu, G., Yu, D., McLeish, T., Su, Z.G., Shen, Z.Y., 2008. Preparation of hierarchical hollow CaCO3 particles and the application as anticancer drug carrier. J. Am. Chem. Soc. 130 (47), 15808–15810.

Yao, H.J., Zhang, Y.G., Sun, L., Liu, Y., 2014. The effect of hyaluronic acid functionalized carbon nanotubes loaded with salinomycin on gastric cancer stem cells. Biomaterials 35 (33), 9208–9223.

Zeng, S., Pöttler, M., Lan, B., Grützmann, R., Pilarsky, C., Yang, H., 2019. Chemoresistance in pancreatic cancer. Int. J. Mol. Sci. 20 (18).

Zhan, Y., Jiang, L., Jin, X., Ying, S., Wu, Z., Wang, L., Yu, W., Tong, J., Zhang, L., Lou, Y., Qiu, Y., 2021. Inhibiting RRM2 to enhance the anticancer activity of chemotherapy. Biomed. Pharmacother. 133, 110996.

Zhao, P., Tian, Y., You, J., Hu, X., Liu, Y., 2022. Recent Advances of Calcium Carbonate Nanoparticles for Biomedical Applications. Bioengineering (Basel) 9 (11).

Zhao, Y., Zheng, Y., Zhu, Y., Zhang, Y., Zhu, H., Liu, T., 2021. M1 Macrophage-derived exosomes loaded with gemcitabine and deferasirox against chemoresistant pancreatic cancer. Pharmaceutics 13 (9).

Zhou, H., Wang, W., Hu, H., Ni, X., Ni, S., Xu, Y., Yang, L., Xu, D., 2019. Co-precipitation of calcium carbonate and curcumin in an ethanol medium as a novel approach for curcumin dissolution enhancement. J. Drug Delivery Sci. Technol. 51, 397–402.

Zinzi, L., Contino, M., Cantore, M., Capparelli, E., Leopoldo, M., Colabufo, N.A., 2014. ABC transporters in CSCs membranes as a novel target for treating tumor relapse. Front. Pharmacol. 5, 163.